Article

Reversible CO₂ Capture and On-Demand Release by an Acidity-Matched Organic Photoswitch

Abdulrahman M. Alfaraidi, Bryan Kudisch, Nina Ni, Jayden Thomas, Thomas Y. George, Khashayar Rajabimoghadam, Haihui Joy Jiang, Daniel G. Nocera, Michael J. Aziz, and Richard Y. Liu*
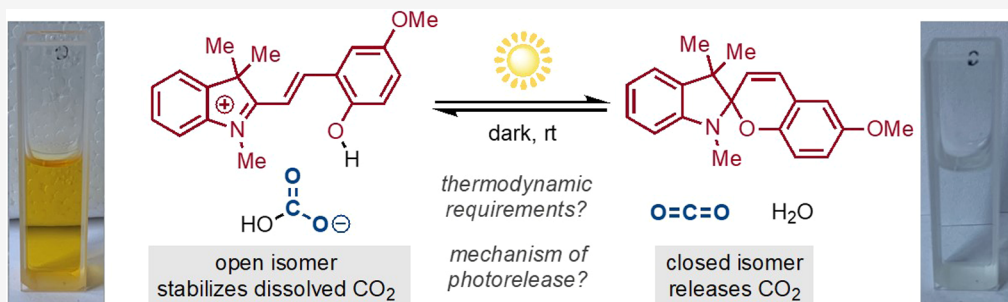
Read Online

ACCESS | Metrics & More | Article Recommendations | Supporting Information

ABSTRACT: Separation of carbon dioxide (CO_2) from point sources or directly from the atmosphere can contribute crucially to climate change mitigation plans in the coming decades. A fundamental practical limitation for the current strategies is the considerable energy cost required to regenerate the sorbent and release the captured CO_2 for storage or utilization. A directly photochemically driven system that demonstrates efficient passive capture and on-demand CO_2 release triggered by sunlight as the sole external stimulus would provide an attractive alternative. However, little is known about the thermodynamic requirements for such a process or mechanisms for modulating the stability of CO_2-derived dissolved species by using photoinduced metastable states. Here, we show that an organic photoswitchable molecule of precisely tuned effective acidity can repeatedly capture and release a near-stoichiometric quantity of CO_2 according to dark−light cycles. The CO_2-derived species rests as a solvent-separated ion pair, and key aspects of its excited-state dynamics that regulate the photorelease efficiency are characterized by transient absorption spectroscopy. The thermodynamic and kinetic concepts established herein will serve as guiding principles for the development of viable solar-powered negative emission technologies.

INTRODUCTION

The accumulation of CO_2 in the atmosphere is a primary driver of anthropogenic climate change, and a dramatic reduction of net emissions is urgently required to avoid catastrophic future scenarios.[1−4] Accordingly, considerable research effort has been dedicated to chemical systems for removing CO_2 from emission streams (CCS, carbon capture and storage)[5,6] and, more recently, from the atmosphere (DAC, direct air capture).[7,8] The most developed technologies for CO_2 capture depend on sorbents such as alkaline aqueous solutions[9] and amines such as ethanolamine,[10] which generally use energy-demanding thermal stripping to release the captured CO_2 for storage and sorbent regeneration (Figure 1A).[11] Complementary approaches using swings in electrical potential[12−14] or applied pressure[15,16] to cycle between capture and release have also been investigated. The viability of these mitigation strategies on scale will likely require that their significant energy demand be ultimately supplied by renewable electricity. As an alternative, we considered whether a chemistry can be devised that directly couples CO_2 capture and release to visible light as the only external energy input.

Such a system could be directly powered by sunlight, for example, according to the day−night cycle and distributed without requiring renewable electricity as an intermediary, along with the costs and limitations associated with its production, storage, distribution, and infrastructure maintenance.

Here, we show that photoswitchable organic molecules can effectively and repeatedly capture CO_2 from the gas phase and release it on demand upon visible-light exposure. Our study focuses on the well-known spiropyran photochromic dyes,[17−19] which can be toggled between two forms, a closed spiropyran isomer **SP** and an open merocyanine isomer **MC**, which differ significantly in chemical properties such as color, acidity, and
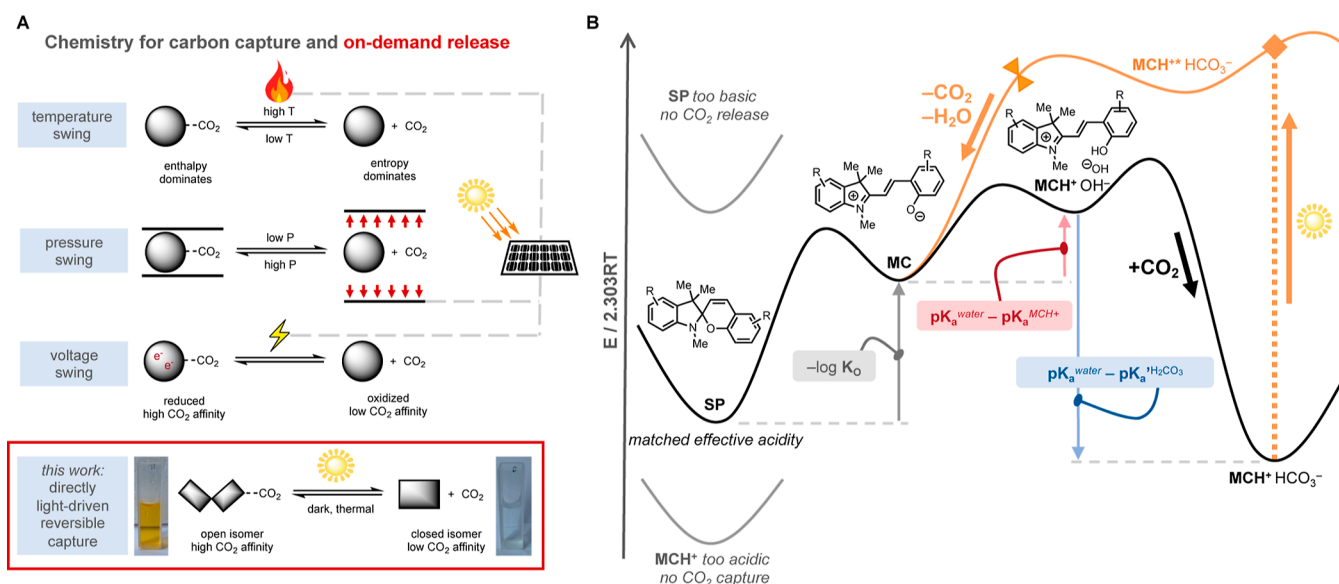
Figure 1. Carbon capture and phototriggered release. (A) Comparison of previously developed chemical processes for reversible CO_2 binding and the new approach in our work. (B) Mechanism for coupling CO_2 capture with photoisomerization of spiropyrans and the required thermodynamic balance. The orange curve shows the excited-state surface reached by MCH^+ upon excitation with visible light. Compounds for which MCH^+ is too acidic (**SP** low in energy) will never have MCH^+ HCO_3^- as the most stable state and therefore will not capture CO_2 effectively. Compounds for which the **SP** form is too basic (**SP** high in energy) will not release CO_2 effectively as an impractically high intensity of light will be required to excite enough MCH^+ to release CO_2 at a rate that competes with its recapture.

metal affinity. In particular, protonated merocyanine (MCH^+) has been shown to engender large, light-driven pH swings[20-22] upon irradiation by releasing its proton and cyclizing to **SP**, which is followed by gradual thermal reversion to its original state. By coupling this photoinduced equilibrium shift with bicarbonate protonation and carbonic acid dehydration equilibria, we envisioned a system that can sequester CO_2 in the dark but changes its resting state to release that CO_2 upon light exposure. Previous research has demonstrated photoacid-triggered formation of carbonic acid for spectroscopic characterization[23] and photoacid-accelerated CO_2 release from acidic conditions.[24] Very recently, an elegant strategy using an indazole photoacid to promote CO_2 release from amino acid sorbents was also reported.[25] However, identification of a single-component solute that can recurrently capture and release according to dark/light cycles remains a highly desirable goal. Further, a systematic framework for analyzing the thermodynamic requirements and experimental investigation of the precise mechanism of the photochemical process is needed to provide a theoretical foundation for the development of this novel approach to reversible carbon capture.
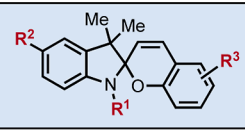
RESULTS AND DISCUSSION

For the proposed process (Figure 1B), a detailed treatment of the thermodynamic balance shows that precise acidity tuning is critical for the realization of the efficient capture and photorelease of CO_2. In solution, a spiropyran **SP** interconverts with an open merocyanine isomer **MC** with an equilibrium constant K_O, which is typically below unity (favoring **SP**) in aqueous environments[26] (for some discussion of solvent effects, see Supporting Information). Because **MC** features a phenoxide moiety, it can act as a base in an aqueous solution and reversibly deprotonate water to form MCH^+ OH^-. The hydroxide anion can sequester dissolved CO_2 as bicarbonate. If capture is to be a spontaneous process, we require MCH^+
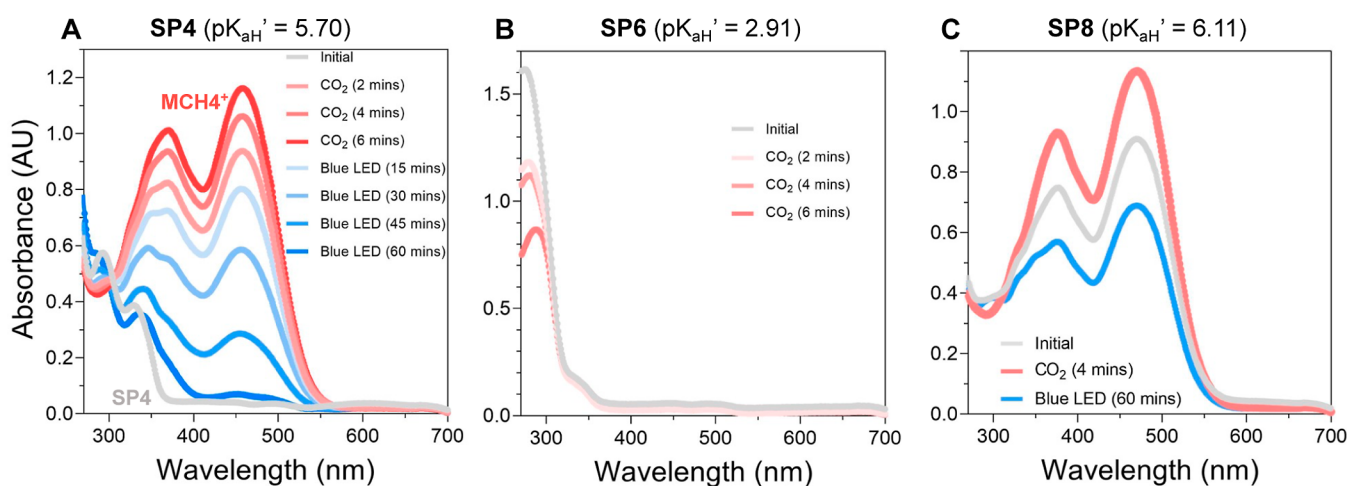
HCO_3^- to be the lowest-energy state in the absence of an external energy input. Upon irradiation, some MCH^+ ions will enter an excited state, the high potential energy of which accelerates reversion to **SP** and/or **MC** with the release of CO_2 and H_2O. For effective release of CO_2 to occur, irradiation must create a sufficient population of MCH^{+*} HCO_3^- such that the net rate of CO_2 release from these excited states can compete with thermal recapture of CO_2. This is difficult to achieve if the relative free energy of **SP** is too high, in which case reversion will require an impractically high intensity of light. A balanced energetic landscape corresponding to optimal photoswitching of uptake and release of CO_2 occurs around (see the Supporting Information for discussion)

$$pK_{aH}'(SP) = pK_a(MCH^+) - \log(1 + K_O^{-1})$$

$$\cong pK_a(H_2CO_3)$$

The quantity on the left represents the apparent conjugate acidity of the spiropyran,[27] $pK_{aH}'(SP)$, which accounts for both the Brønsted acidity of the phenol and the driving force for ring closure. This is an analogue of the classical Henderson–Hasselbalch equation. The optimal balance of capture and photorelease efficiency should be achieved only by molecules for which $pK_{aH}'(SP)$ nears the effective pK_a' of H_2CO_3 in its relevant conditions (6.35 in water,[28] although ion-pairing interactions can alter the exact target value, see below).

To validate this analysis, we synthesized spiropyrans **SP1**–**SP8** (Figure 2), varying in substitution on nitrogen (R^1) and C5 (R^2) of the indoline, as well as on the chromene fragment ortho and para to the oxygen (R^3). These spiropyran structures can be easily accessed on a gram-to-kilogram scale,[29-31] usually in a single step from commercial materials. The effective pK_{aH}' values of these molecules in 1:1 DMSO/water were determined by spectrophotometric titration, using the moderate UV absorbance of **SP** and the strong UV-to-visible

|	R¹	R²	R³	λ_{MCH+} (nm) [ε_{MCH+} (M⁻¹ cm⁻¹)]	λ_{SP} (nm)	pK$_{aH}$'
SP1	Me	H	H	424 [21,750]	289	5.35
SP2	Me	H	p-Me	438 [19,270]	273	5.23
SP3	Me	H	o-OMe	401 [16,100]	291	5.51
SP4	Me	H	p-OMe	460 [22,080]	291	5.70
SP5	Me	H	p-NMe₂	388 [16,000]	291	5.62
SP6	Me	CN	p-OMe	482 [7,500]	288	2.91
SP7	(CH₂)₃SO₃⁻	H	o-OMe	396 [24,333]	278	6.05
SP8	(CH₂)₃SO₃⁻	H	p-OMe	468 [19,900]	296	6.11

Figure 2. Spiropyrans: properties and response to CO_2 and light exposure. (top) Summary of spiropyrans evaluated in this work with effective acidities shown on the right. (A) An acidity-matched spiropyran **SP4** captures CO_2 rapidly to generate **MCH4⁺** and converts back to its original spiropyran form, releasing CO_2 during irradiation with 450 nm light. (B) Spiropyran **SP6** that is too acidic and therefore does not generate **MCH6⁺** in the presence of CO_2. (C) Spiropyran **SP8** that is too basic and already exists in its merocyanine form **MCH8⁺** in neutral solution. This material captures CO_2 but does not undergo efficient photorelease. This compound is synthesized in the −SO₃H form, and the presence of this acidic group can contribute to the initial protonation state.

absorbance of **MCH⁺** generated upon isomerization and protonation of **SP**. The parent spiropyran **SP1** is moderately basic (pK$_{aH}$' = 5.30) in its ground state, and the installation of electron-donating groups on the chromene unit results in the expected increase in basicity of the phenoxide, elevating the pK$_{aH}$' of **SP3** (R³ = o-OCH₃, pK$_{aH}$' = 5.51), **SP4** (R³ = p-OCH₃, pK$_{aH}$' = 5.70), and **SP5** (R³ = p-N(CH₃)₂, pK$_{aH}$' = 5.62) relative to that of **SP1**. An electron-withdrawing group on the indoline of **SP6** (R² = CN), while likely imparting minimal influence on the phenoxide basicity, greatly enhances the effective acidity (pK$_{aH}$' = 2.91) of the corresponding protonated merocyanine form by favoring the closed, spiropyran form (lowering K$_O$). The attachment of a solubilizing sulfonate chain on the indoline nitrogen was found to reduce the effective acidity, presumably due to electrostatic effects, as exemplified by **SP7** (R¹ = (CH₂)₃SO₃⁻, R³ = o-OCH₃, and pK$_{aH}$' = 6.05) and **SP8** (R¹ = (CH₂)₃SO₃⁻, R³ = p-OCH₃, and pK$_{aH}$' = 6.11).

DMSO−water solutions containing these spiropyrans were evaluated for their competence in the capture of gaseous CO_2 and subsequent release under visible-light irradiation. The range of effective acidities represented by our panel of

analogues allowed us to experimentally confirm our acidity-matching hypothesis, which states that there is an optimal pK$_{aH}$' for switchable binding to CO_2. In accordance with these predictions, for the most acidic photochromes such as **SP6** (pK$_{aH}$' = 2.91), exposure to pure CO_2 (1 atm) did not result in any formation of the corresponding protonated merocyanine **MCH6⁺** (λ_{max} = 482 nm, Figure 2B). Conversely, the most basic photochromes such as **SP8** (pK$_{aH}$' = 6.11), when dissolved in 1:1 DMSO/water, exist significantly in their open isomer **MCH8⁺** form (λ_{max} = 468 nm) due to their ability to reversibly deprotonate water (Figure 2C). Although exposure to pure CO_2 (1 atm) resulted in only a minor increase in the observed quantity of **MCH8⁺**, a significant amount of CO_2 capture was indicated by the change in pH of the solution from 7.8 to 5.3 (Figure S32). For compounds that exist significantly in the **MCH⁺** form in solution, the extent of CO_2 capture is difficult to infer from spectrophotometry alone as the UV−vis absorbance spectrum primarily reflects the concentration of the merocyanine-derived cation and is essentially independent of the anion. As anticipated, **MCH8⁺** HCO₃⁻ is extremely stable, and irradiation by blue LEDs (λ_{max} = 450 nm) resulted in a relatively small change in the spectrum and a 0.7 pH unit
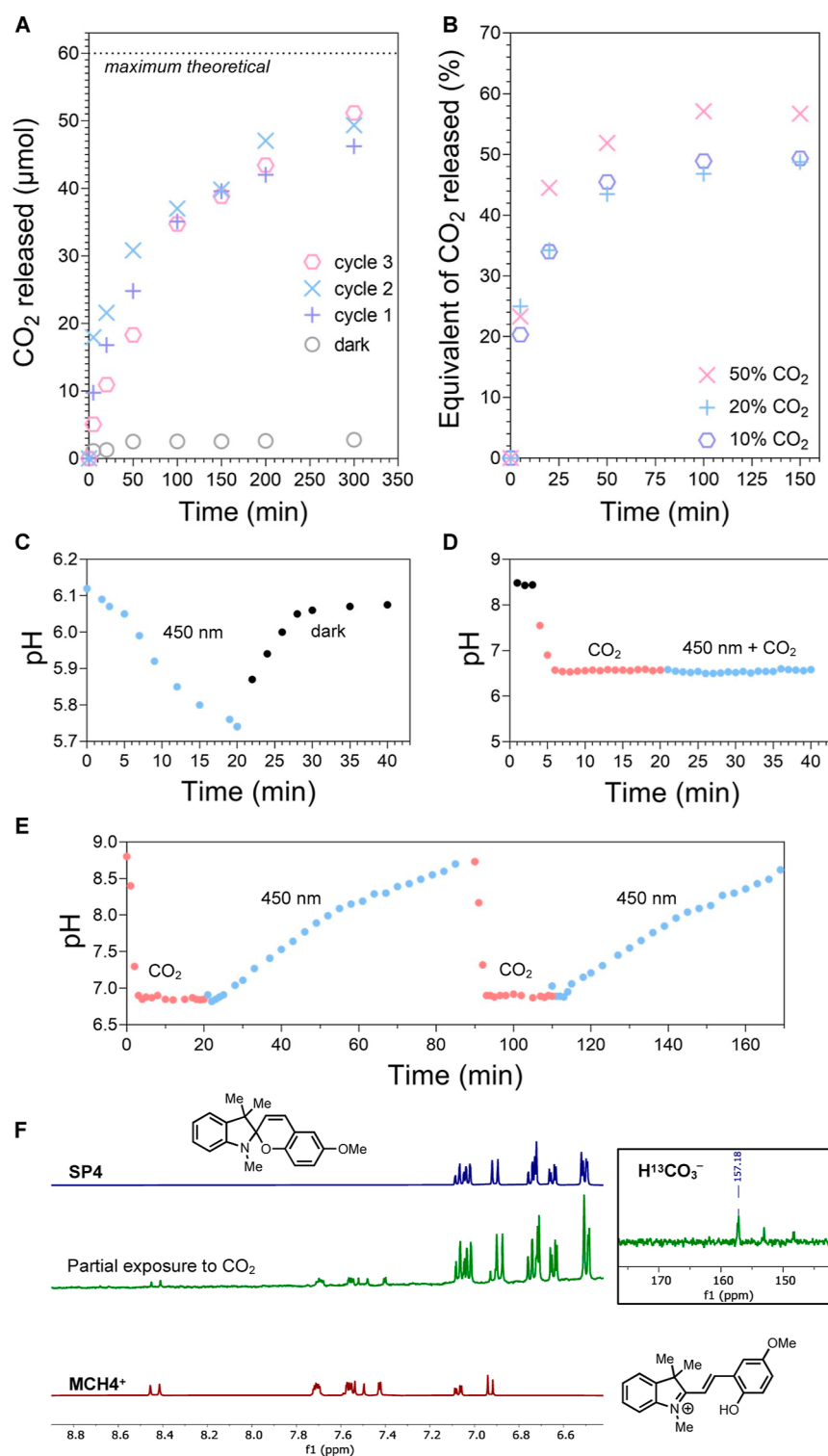
Figure 3. CO₂ passive capture and photorelease: performance and mechanism. (A) GC quantification of the released CO_2 from three consecutive cycles of exposure to CO_2 and blue-light (450 nm) irradiation, including a control replicate performed with the sample shielded by reflective foil. (B) Released CO_2 after capture from CO_2/N_2 mixtures. In situ pH tracking of a DMSO−water solution of 5 mM **SP4** (C) during irradiation and in the dark with initial adjusted pH set to 6.1 to partially convert **SP4** to the **MCH4⁺** Cl⁻ form, (D) during irradiation of the sample while overhead pressure of CO_2 was maintained, and (E) during CO_2 capture and photochemical release. (F) NMR spectroscopic evidence for **MCH4⁺** HCO_3^- as the resting state of the captured CO_2.

increase even after 60 min, reflecting negligible CO_2 release. These negative examples contrast dramatically with the promising results obtained using compounds of moderate acidity such as **SP4** ($pK_{aH}' = 5.70$) and, to a lesser extent, **SP2**

($pK_a' = 5.23$). For example (Figure 2A), exposure of **SP4** to pure CO_2 (1 atm) resulted in rapid and isosbestic conversion to **MCH4⁺**, which, at this stage, we hypothesized to be paired to HCO_3^-. We proceeded to irradiate this solution with 450
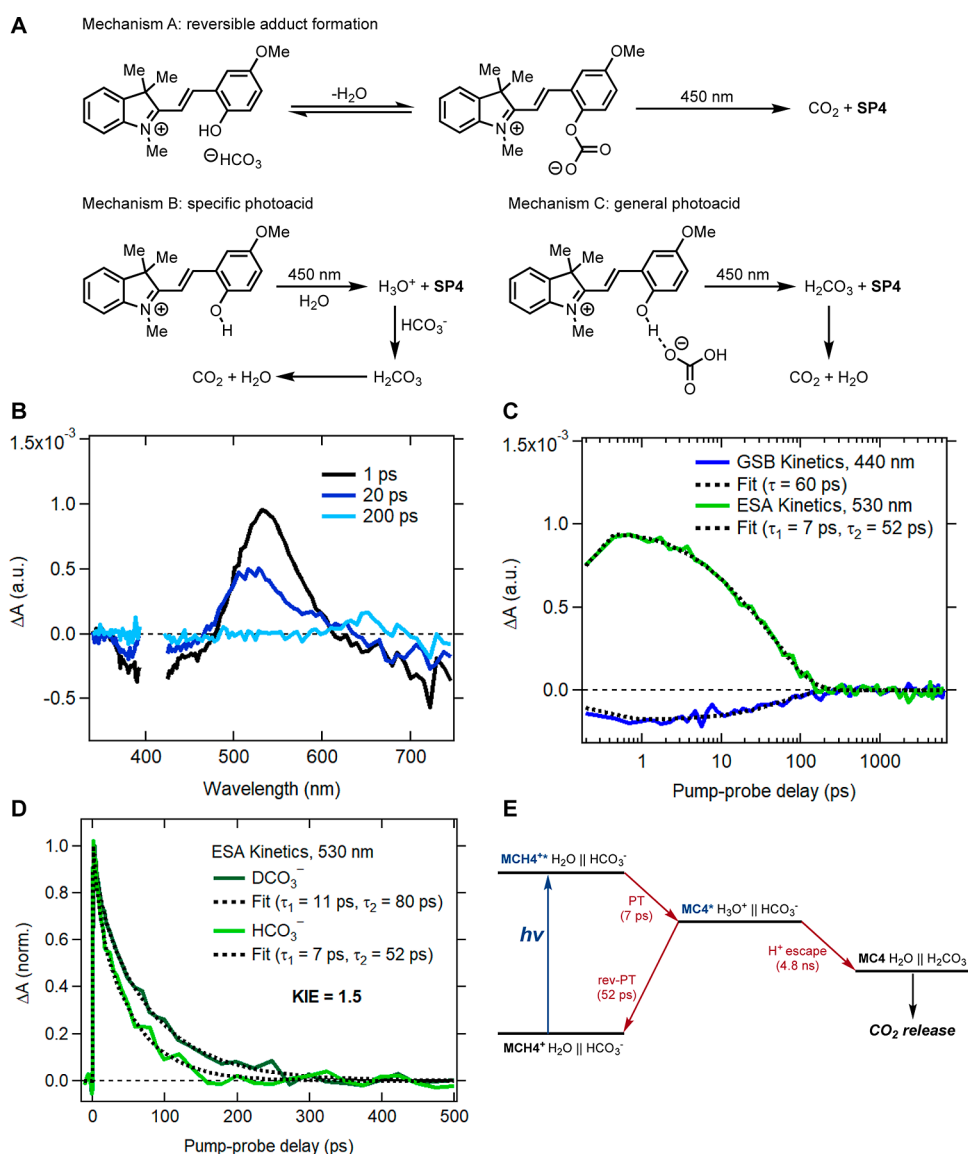
Figure 4. Mechanism of CO_2 photorelease. (A) Three mechanistic proposals considered in this study. (B) Transient absorption spectra of **MCH4**$^+$ HCO_3^-, with excitation at 400 nm. The laser scattering region was removed for clarity. (C) Decay kinetics of the ground-state bleach and ESA features with exponential and biexponential fits, respectively. (D) Comparative decay profiles of the ESA using **MCH4**$^+$ HCO_3^- and **MCD4**$^+$ DCO_3^-, showing a KIE of ~1.5 for both processes represented in the biexponential kinetic model. (E) Proposed scheme for CO_2 release after initial electronic excitation of **MCH4**$^+$. Ions divided by double vertical lines indicate a solvent-separated ion pair, in which the ions are not directly in contact but separated by a few enough solvent molecules that the anion still exerts a detectable influence on the reactivity of the cation.

nm blue light, upon which the disappearance of **MCH4**$^+$ occurred, accompanied by a complete recovery of the original spectrum. Similar but slower conversion in both directions was observed with **SP2** (Figure S9). This compound is also significantly less soluble than **SP4** (26 mM vs < 2 mM for **SP2**), so we elected to proceed with **SP4** for the ensuing analysis.

Successful repeated capture and light-triggered release of CO_2 by **SP4** were confirmed by quantitative gas chromatography (GC) calibrated against standard mixtures (Figure 3A). After the introduction of CO_2 into a solution of **SP4** (60 μmol in 3 mL of solvent, 4:1 DMSO/water), which elicited the appearance of an intense yellow color, the vial headspace was replaced with nitrogen, and the cuvette was exposed to 450 nm light. Aliquots of the gas in the headspace were analyzed, and the gaseous CO_2 content was observed to increase over time (half-life of ca. 60 min) to a terminal value of 46–51 μmol,

representing on average 81% of theoretical capture capacity. The now-colorless solution was then immediately re-exposed to CO_2, and the photorelease procedure was performed again for a total of three capture-release cycles. No difference in activity was observed, implying that the spiropyran dye shows stability under these operating conditions, including extended exposure to atmospheric oxygen, which is not tolerated by most molecular redox approaches. Temperature control during irradiation was carefully maintained using portable fans, and control experiments in which the sample was shielded from light by reflective foil displayed a negligible release of CO_2. Spectrophotometry further confirmed that release in the dark is extremely slow even when opened to the atmosphere (11.5% decrease in **MCH4**$^+$ HCO_3^- over 9 h, Figure S13). Pure gas input was not required for capture (Figure 3B): using 50%, 20%, and 10% (v/v) mixtures of CO_2 in N_2 delivered similar results, although the total quantity of CO_2 released relative to

SP4 decreased to roughly 50% in the most dilute case. Nevertheless, these experiments prove the concept of cyclic carbon capture and release using visible light as the only external energy input.

To further illustrate key mechanistic aspects of the capture and release processes, in situ pH tracking experiments were conducted (Figure 3C−E), which revealed a shift between pH-determining species resulting from the coupling of multiple equilibria. First, hydrochloric acid was added to partially convert **SP4** to the **MCH4⁺ Cl⁻** form. The protonated cation is a metastable-state photoacid that, upon irradiation, converts to **SP4** while releasing a proton to the solvent, and accordingly, a decrease in the pH was measured. Upon removal of the light source, the pH rapidly recovered to its starting value, as **SP4** thermally reverts to **MC4**, which is rapidly reprotonated. If instead of using a strong acid, equilibration with an atmosphere of CO_2 was used to open **SP4** to its protonated merocyanine form, identical irradiation conditions resulted in no noticeable change in pH provided that the solution remained in equilibrium with an applied pressure of CO_2. This difference is due to the buffering capacity of bicarbonate as the photoreaction of **MCH4⁺** now prompts net proton transfer to bicarbonate rather than the solvent and therefore cannot be perceived by pH measurement. Under a headspace of pure CO_2, dissolved CO_2 remains in solution and can quickly reprotonate **SP4** via carbonic acid. If the CO_2-charged solution is opened to the air such that CO_2 formed from protonation and dehydration of bicarbonate can escape, photoirradiation results in a steady increase in the solution pH. The photoacidic activity of **MCH4⁺** results in a net basification of the solution because the released proton is not received by the solvent but participates with bicarbonate in an irreversible process $\left(H_2CO_{3(aq)} \rightarrow H_2O_{(l)} + CO_{2(g)}\right)$ that depletes carbonic acid, which has the effect of decreasing the total concentration of dissolved acidic species. Although the CO_2 outgassing process formally exchanges a higher pK_a buffer $\left(CO_2/HCO_3^-\right)$ for a lower pK_a buffer (**MCH4⁺/SP4**), which one might expect to lead to acidification, there is a concomitant shift in the protonation state of the buffer as carbonic acid is converted into less acidic species $\left(H_2O_{(l)} + CO_{2(g)}\right)$. The observed rate of CO_2 evolution in the pH-tracking experiments is slightly higher than that recorded in the above GC measurements (Figure 2A), which is due to the pH-tracking being performed fully open to the atmosphere, while the GC study was performed in a sealed vial to accurately quantify gaseous CO_2. Consistent with our model, the pH could be reverted to its starting point with the removal of the light source and equilibration under an atmosphere of CO_2.

The assignment of dominant dissolved inorganic carbon species such as **MCH4⁺ HCO₃⁻**, as opposed to a direct covalent adduct such as **MC4-CO₂**, could not be established on the basis of spectrophotometry alone, as TD-DFT calculations indicate that the lowest-energy excitations are similar in energy for free **MCH4⁺** (497 nm), **MCH4⁺...HCO₃⁻** (509 nm), and **MC4-CO₂** (473 nm), and all are close to the experimental λ_{max} (460 nm). However, the identity of the cation as **MCH4⁺** is apparent from ¹H NMR spectroscopy (Figure 3F): the protonated merocyanine could be independently prepared by protonation of **SP4** with strong acid, and partial exposure of **SP4** to gaseous CO_2 resulted in the evolution of identical resonances in the ¹H NMR. When this same spiropyran was exposed to ¹³C-labeled CO_2, a broad resonance arose in the ¹³C NMR spectrum at a chemical shift

of 157.2 ppm, which is likely associated with [¹³C]-bicarbonate.

Having established the relevant ground-state structures involved in the light-driven capture cycle, we turned to further dissecting the mechanism of the photorelease subprocess. Three plausible pathways were considered (Figure 4A): (A) a nonphotoacid mechanism, involving reversible formation of the adduct **MC4-CO₂** and subsequent photoinduced cleavage of the O−CO₂⁻ bond; (B) a specific photoacid mechanism, in which **MCH4⁺** releases its proton to water upon irradiation, and the solvent serves to transfer this proton to a separated or distant HCO_3^- to form carbonic acid; and (C) a general photoacid mechanism, in which **MCH4⁺** and HCO_3^- as a contact ion pair directly exchange a proton in the excited state.

A solution containing **MCH4⁺ HCO₃⁻** was prepared by bubbling CO_2 into dissolved **SP4**, and the excited-state dynamics of this species were investigated by ultrafast transient absorption spectroscopy (Figure 4B). After excitation using a 400 nm laser pulse, significant excited-state absorption (ESA) was observed at 530 nm. We assigned this feature to **MC4*** obtained upon the deprotonation of **MCH4⁺*** in its excited state. The transient bleach above 600 nm is likely due to stimulated emission from **MC4*** (Figure S39). The decay of ESA intensity at 530 nm fits well with a biexponential function with time constants τ_1 = 7 ps and τ_2 = 52 ps (Figure 4C), with relative amplitudes of 0.23 and 0.77, respectively. As examined further below, we propose these first-order decays are associated with proton-transfer (PT) and reverse-proton-transfer (rev-PT) processes from **MCH4⁺** to water.

A significant kinetic isotope effect (KIE) was observed in the rates of both steps by using D_2O as an alternative solvent (τ_1 = 7 ps using H_2O vs τ_1 = 11 ps using D_2O, KIE = 1.6; τ_2 = 52 ps using H_2O vs τ_2 = 80 ps using D_2O, KIE = 1.5, Figure 4D; and the relative amplitudes of the two exponentials in D_2O were 0.2 and 0.8, respectively). The magnitudes of these deuterium isotope effects are potentially consistent with proton transfer between two heteroatomic sites of widely differing acidities (mechanisms B and C). These results would be more difficult to rationalize in a nonphotoacid pathway such as mechanism A, in which no primary isotope effect should manifest. The same transient absorption experiments were also repeated with **MCH4⁺ Cl⁻** and **MCD4⁺ Cl⁻**, and time constants (τ_1 = 5 ps using HCl vs τ_1 = 12 ps using DCl, KIE = 2.4; τ_2 = 46 ps using HCl vs τ_2 = 73 ps using DCl, KIE = 1.6) were found to be similar to those measured with bicarbonate (Figure S36), suggesting that the initial acceptor of the merocyanine-derived proton was not the anion. This observation led us to favor mechanism B, in which the immediate target is a solvent (water) molecule.

Figure 4E summarizes the proposed overall scheme for light-driven generation of carbonic acid from **MCH4⁺ HCO₃⁻**. After photoexcitation of **MCH4⁺**, rapid proton transfer (τ = 7 ps) takes place from the merocyanine to a hydrogen-bonded water molecule with minimal heavy-atom motion, forming a hydrogen-bonded excited-state complex [**MC4*...H₃O⁺**]. This complex can either undergo reverse proton transfer (τ = 52 ps) to restore the initial **MCH4⁺**, or the proton can diffuse away through a von Grotthuss-type mechanism[32−34] to find a basic bicarbonate anion. Based on a quantum yield of 1.3% for the formation of **MC4** derived from nanosecond transient absorption spectroscopy, the proton escape takes place on the order of ca. 4.8 ns. Higher proton-escape quantum yields (50%) have been observed from other protonated

merocyanines that are stronger photoacids,[35,36] as estimated based on their transient absorption spectra. These observations give us encouragement that the development of more efficient photoacids for bicarbonate protonation is possible and that the rationale for the difference between our photoacids and previous examples continues to be investigated.

Interestingly, when the sample was prepared such that the anion was chloride instead of bicarbonate, we found a minor but verifiable decrease in the quantum yield (1.1%), indicating the likely involvement of the counteranion in regulating competition between the reverse-proton-transfer and proton-escape pathways. Thus, the nature of **MCH4$^+$ HCO$_3^-$** under these conditions is most aptly described as a solvent-separated ion pair,[37,38] rather than as free ions. The electrostatically associated bicarbonate is not the direct recipient of the proton from **MCH4$^+$** but does remain sufficiently proximal to influence the preorganization of the intervening solvent molecule(s) and, thereby, the frequency of carbonic acid formation. If accurate, then this scheme is informative for optimizing the rate of CO_2 photogeneration. For example, structural modifications that promote dissociation of hydronium from the **MC4...H$_3$O$^+$** complex might reduce the rate of reverse proton transfer, while strengthening the attractive interactions between **MCH4$^+$** and HCO$_3^-$ should accelerate the productive protonation of bicarbonate.

CONCLUSIONS

In conclusion, this work demonstrates repeated, on-demand CO_2 capture and release using photoswitchable acids. A systematic assessment of structure−activity relationships underscores the importance of effective-acidity tuning in achieving efficient cycling. Ultrafast spectroscopy and KIEs suggest a solvent-separated ion pair mechanism for photo-release, a theory that can guide the development of more efficient photoacid structures. Studies into implementing these design principles and other modifications aimed at maximizing solubility, synthetic scalability, longevity, and wavelength coverage are ongoing with the long-term intention of generalizing solar-powered carbon removal technologies.

ASSOCIATED CONTENT

Ⓢ Supporting Information

The Supporting Information is available free of charge at https://pubs.acs.org/doi/10.1021/jacs.3c08471.

> Experimental methods, synthetic procedures, spectroscopic data, computational results, and additional discussion and references (PDF)

AUTHOR INFORMATION

Corresponding Author

Richard Y. Liu − *Department of Chemistry and Chemical Biology, Harvard University, Cambridge, Massachusetts 02138, United States;* ⦿ orcid.org/0000-0003-0951-6487; Email: richardliu@chemistry.harvard.edu

Authors

Abdulrahman M. Alfaraidi − *Department of Chemistry and Chemical Biology, Harvard University, Cambridge, Massachusetts 02138, United States*

Bryan Kudisch − *Department of Chemistry and Chemical Biology, Harvard University, Cambridge, Massachusetts 02138, United States;* ⦿ orcid.org/0000-0003-3352-5383

Nina Ni − *Department of Chemistry and Chemical Biology, Harvard University, Cambridge, Massachusetts 02138, United States*

Jayden Thomas − *Department of Chemistry and Chemical Biology, Harvard University, Cambridge, Massachusetts 02138, United States*

Thomas Y. George − *Harvard John A. Paulson School of Engineering and Applied Sciences, Cambridge, Massachusetts 02138, United States;* ⦿ orcid.org/0000-0002-0159-8521

Khashayar Rajabimoghadam − *Department of Chemistry and Chemical Biology, Harvard University, Cambridge, Massachusetts 02138, United States*

Haihui Joy Jiang − *Department of Chemistry and Chemical Biology, Harvard University, Cambridge, Massachusetts 02138, United States;* ⦿ orcid.org/0000-0002-7302-755X

Daniel G. Nocera − *Department of Chemistry and Chemical Biology, Harvard University, Cambridge, Massachusetts 02138, United States;* ⦿ orcid.org/0000-0001-5055-320X

Michael J. Aziz − *Harvard John A. Paulson School of Engineering and Applied Sciences, Cambridge, Massachusetts 02138, United States;* ⦿ orcid.org/0000-0001-9657-9456

Complete contact information is available at:
https://pubs.acs.org/10.1021/jacs.3c08471

Notes

The authors declare no competing financial interest.

ACKNOWLEDGMENTS

REFERENCES

(1) Minx, J. C.; Lamb, W. F.; Callaghan, M. W.; Fuss, S.; Hilaire, J.; Creutzig, F.; Amann, T.; Beringer, T.; de Oliveira Garcia, W.; Hartmann, J.; Khanna, T.; Lenzi, D.; Luderer, G.; Nemet, G. F.; Rogelj, J.; Smith, P.; Vicente Vicente, J. L.; Wilcox, J.; del Mar Zamora Dominguez, M. Negative Emissions Part 1: Research Landscape and Synthesis. *Environ. Res. Lett.* **2018**, *13* (6), 063001.

(2) Masson-Delmotte, V.; Zhai, P.; Pirani, A.; Connors, S. L.; Péan, C.; Chen, Y.; Goldfarb, L.; Gomis, M. I.; Matthews, R.; Berger, S.; Huang, M.; Yelekçi, O.; Yu, R.; Zhou, B.; Lonnoy, E.; Maycock, T. K.; Waterfield, T.; Leitzell, K.; Caud, N. *Climate Change 2021: The Physical Science Basis: Contribution of Working Group I to the Sixth Assessment Report of the Intergovernmental Panel on Climate Change;* IPCC; Intergovernmental Panel on Climate Change: Cambridge University Press, Cambridge, United Kingdom and New York, NY, USA, 2021.

(3) Edenhofer, O.; Pichs-Madruga, R.; Sokona, Y.; Minx, J. C.; Farahani, E.; Kadner, S.; Seyboth, K.; Adler, A.; Baum, I.; Brunner, S.; Eickemeier, P.; Kriemann, B.; Savolainen, J.; Schlömer, S.; von Stechow, C.; Zwickel, T. *Climate Change 2014: Mitigation of Climate Change: Working Group III Contribution to the Fifth Assessment Report of the Intergovernmental Panel on Climate Change;* IPCC; Inter-

governmental Panel on Climate Change: Cambridge University Press, Cambridge, United Kingdom and New York, NY, USA, 2014. https://www.ipcc.ch/site/assets/uploads/2018/02/ipcc_wg3_ar5_full.pdf.

(4) Giorgi, F.; Whetton, P. H.; Jones, R. G.; Christensen, J. H.; Mearns, L. O.; Hewitson, B.; vonStorch, H.; Francisco, R.; Jack, C. Emerging Patterns of Simulated Regional Climatic Changes for the 21st Century Due to Anthropogenic Forcings. *Geophys. Res. Lett.* **2001**, *28*, 3317−3320.

(5) Leung, D. Y. C.; Caramanna, G.; Maroto-Valer, M. M. An Overview of Current Status of Carbon Dioxide Capture and Storage Technologies. *Renew. Sustain. Energy Rev.* **2014**, *39*, 426−443.

(6) Gibbins, J.; Chalmers, H. Carbon Capture and Storage. *Energy Pol.* **2008**, *36* (12), 4317−4322.

(7) Hanna, R.; Abdulla, A.; Xu, Y.; Victor, D. G. Emergency Deployment of Direct Air Capture as a Response to the Climate Crisis. *Nat. Commun.* **2021**, *12* (1), 368.

(8) Sanz-Pérez, E. S.; Murdock, C. R.; Didas, S. A.; Jones, C. W. Direct Capture of CO2 from Ambient Air. *Chem. Rev.* **2016**, *116* (19), 11840−11876.

(9) Keith, D. W.; Holmes, G.; St. Angelo, D.; Heidel, K. A Process for Capturing CO2 from the Atmosphere. *Joule* **2018**, *2* (8), 1573−1594.

(10) Rochelle, G. T. Amine Scrubbing for CO2 Capture. *Science* **2009**, *325* (5948), 1652−1654.

(11) Mazari, S. A.; Si Ali, B.; Jan, B. M.; Saeed, I. M.; Nizamuddin, S. An Overview of Solvent Management and Emissions of Amine-Based CO2 Capture Technology. *Int. J. Greenh. Gas Control* **2015**, *34*, 129−140.

(12) Jin, S.; Wu, M.; Gordon, R. G.; Aziz, M. J.; Kwabi, D. G. PH Swing Cycle for CO2 Capture Electrochemically Driven through Proton-Coupled Electron Transfer. *Energy Environ. Sci.* **2020**, *13* (10), 3706−3722.

(13) Voskian, S.; Hatton, T. A. Faradaic Electro-Swing Reactive Adsorption for CO2 Capture. *Energy Environ. Sci.* **2019**, *12* (12), 3530−3547.

(14) Sharifian, R.; Wagterveld, R. M.; Digdaya, I. A.; Xiang, C.; Vermaas, D. A. Electrochemical Carbon Dioxide Capture to Close the Carbon Cycle. *Energy Environ. Sci.* **2021**, *14* (2), 781−814.

(15) Ho, M. T.; Allinson, G. W.; Wiley, D. E. Reducing the Cost of CO2 Capture from Flue Gases Using Pressure Swing Adsorption. *Ind. Eng. Chem. Res.* **2008**, *47*, 4883−4890.

(16) Siqueira, R. M.; Freitas, G. R.; Peixoto, H. R.; Nascimento, J. F. d.; Musse, A. P. S.; Torres, A. E. B.; Azevedo, D. C. S.; Bastos-Neto, M. Carbon Dioxide Capture by Pressure Swing Adsorption. *Energy Procedia* **2017**, *114*, 2182−2192.

(17) Kortekaas, L.; Browne, W. R. The Evolution of Spiropyran: Fundamentals and Progress of an Extraordinarily Versatile Photochrome. *Chem. Soc. Rev.* **2019**, *48* (12), 3406−3424.

(18) Klajn, R. Spiropyran-Based Dynamic Materials. *Chem. Soc. Rev.* **2014**, *43* (1), 148−184.

(19) Liao, Y. Design and Applications of Metastable-State Photoacids. *Acc. Chem. Res.* **2017**, *50* (8), 1956−1964.

(20) Wimberger, L.; Prasad, S. K. K.; Peeks, M. D.; Andréasson, J.; Schmidt, T. W.; Beves, J. E. Large, Tunable, and Reversible PH Changes by Merocyanine Photoacids. *J. Am. Chem. Soc.* **2021**, *143* (49), 20758−20768.

(21) Berton, C.; Busiello, D. M.; Zamuner, S.; Scopelliti, R.; Fadaei-Tirani, F.; Severin, K.; Pezzato, C. Light-Switchable Buffers. *Angew. Chem., Int. Ed.* **2021**, *60* (40), 21737−21740.

(22) Wimberger, L.; Andréasson, J.; Beves, J. E. Basic-to-Acidic Reversible PH Switching with a Merocyanine Photoacid. *Chem. Commun.* **2022**, *58* (37), 5610−5613.

(23) Adamczyk, K.; Prémont-Schwarz, M.; Pines, D.; Pines, E.; Nibbering, E. T. J. Real-Time Observation of Carbonic Acid Formation in Aqueous Solution. *Science* **2009**, *326* (5960), 1690−1694.

(24) Bennett, R.; Clifford, S.; Anderson, K.; Puxty, G. Carbon Capture Powered by Solar Energy. *Energy Proc.* **2017**, *114*, 1−6.

(25) Premadasa, U. I.; Bocharova, V.; Miles, A. R.; Stamberga, D.; Belony, S.; Bryantsev, V. S.; Elgattar, A.; Liao, Y.; Damron, J. T.; Kidder, M. K.; Doughty, B.; Custelcean, R.; Ma, Y.-Z. Photochemically-Driven CO2 Release Using a Metastable-State Photoacid for Energy Efficient Direct Air Capture. *Angew. Chem., Int. Ed.* **2023**, *62* (29), No. e202304957.

(26) Berton, C.; Pezzato, C. Photoacidity of Indolinospirobenzopyrans in Water. *Eur. J. Org Chem.* **2023**, *26* (17), No. e202300070.

(27) Berton, C.; Busiello, D. M.; Zamuner, S.; Solari, E.; Scopelliti, R.; Fadaei-Tirani, F.; Severin, K.; Pezzato, C. Thermodynamics and Kinetics of Protonated Merocyanine Photoacids in Water. *Chem. Sci.* **2020**, *11* (32), 8457−8468.

(28) Zeebe, R. E.; Wolf-Gladrow, D. *CO₂ in Seawater: Equilibrium, Kinetics, Isotopes*, 1st ed.; Elsevier, 2001.

(29) Barbee, M. H.; Mondal, K.; Deng, J. Z.; Bharambe, V.; Neumann, T. V.; Adams, J. J.; Boechler, N.; Dickey, M. D.; Craig, S. L. Mechanochromic Stretchable Electronics. *ACS Appl. Mater. Interfaces* **2018**, *10* (35), 29918−29924.

(30) Yang, H.; Hu, W.; Sun, C.; Ren, Y.; Qin, S.; Huang, J. Spiropyrane Derivative with Color, Fluorescence and Liquid Crystal Property Triple Switching Effects as Well as Preparation Method and Application Thereof. China Patent CN 113024571 A, 2021.

(31) Wang, M.; Zhang, H.; Ji, L.; Fan, W.; Qiao, Z.; Si, Y.; Wang, Z.; Zheng, Y.; Xue, X.; Wu, X.; Liu, Y. Photochromic Optical Material. China Patent CN 107722028 A, 2018.

(32) Mohammed, O. F.; Pines, D.; Dreyer, J.; Pines, E.; Nibbering, E. T. J. Sequential Proton Transfer Through Water Bridges in Acid-Base Reactions. *Science* **2005**, *310* (5745), 83−86.

(33) Rini, M.; Magnes, B.-Z.; Pines, E.; Nibbering, E. T. J. Real-Time Observation of Bimodal Proton Transfer in Acid-Base Pairs in Water. *Science* **2003**, *301* (5631), 349−352.

(34) Mohammed, O. F.; Pines, D.; Nibbering, E. T. J.; Pines, E. Base-Induced Solvent Switches in Acid-Base Reactions. *Angew. Chem., Int. Ed.* **2007**, *46* (9), 1458−1461.

(35) Kaiser, C.; Halbritter, T.; Heckel, A.; Wachtveitl, J. Proton-Transfer Dynamics of Photoacidic Merocyanines in Aqueous Solution. *Chem.—Eur. J.* **2021**, *27* (35), 9160−9173.

(36) Aldaz, C. R.; Wiley, T. E.; Miller, N. A.; Abeyrathna, N.; Liao, Y.; Zimmerman, P. M.; Sension, R. J. Experimental and Theoretical Characterization of Ultrafast Water-Soluble Photochromic Photoacids. *J. Phys. Chem. B* **2021**, *125* (16), 4120−4131.

(37) Winstein, S.; Clippinger, E.; Fainberg, A. H.; Heck, R.; Robinson, G. C. Salt Effects and Ion Pairs in Solvolysis and Related Reactions. III.[1] Common Ion Rate Depression and Exchange of Anions during Acetolysis[2,3]. *J. Am. Chem. Soc.* **1956**, *78* (2), 328−335.

(38) Bentley, T. W.; von R. Schleyer, P. Medium Effects on the Rates and Mechanisms of Solvolytic Reactions. *Advances in Physical Organic Chemistry*; Gold, V., Ed.; Academic Press, 1977; Vol. 14, pp 1−67..